

Letters

Periodic Arrays of Interfacial Cylindrical Reverse Micelles[†]Mark Nelson,[‡] Nicholas Cain,[‡] Chad E. Taylor,[‡] Benjamin M. Ocko,[§] Douglas L. Gin,[‡] Scott R. Hammond,[‡] and Daniel K. Schwartz^{*,‡}*Department of Chemical and Biological Engineering, University of Colorado, Boulder, Colorado 80309, and Department of Physics, Brookhaven National Laboratory, Upton, New York**Received January 24, 2005. In Final Form: March 28, 2005*

We report an approach for the fabrication of periodic molecular nanostructures on surfaces. The approach involves biomimetic self-organization of synthetic wedge-shaped amphiphilic molecules into multilayer arrays of cylindrical reverse micelles. The films were characterized by atomic force microscopy and X-ray reflectivity. These nanostructured films self-assemble in solution but remain stable upon removal and exposure to ambient conditions, making them potentially suitable for a variety of dry pattern transfer methods. We illustrate the generality of this approach by using two distinct molecular systems that vary in size by a factor of 2.

Introduction

Biomimetic molecular self-organization has become an important and viable method for the creation of nanoscale objects and materials as a result of the potential for massively parallel fabrication of highly uniform (monodisperse) and organized assemblies. The self-organization of natural and synthetic peptides,^{1–3} polynucleotides,^{4–6} diblock copolymers,^{7–10} lipids/surfactants,^{11–14} and combinations of these species^{15,16} has been widely exploited in three dimensions for applications including nanoparticle synthesis, nanocomposite and nanoporous materials, biomaterials, and sensors. Similarly, the ability to control

two-dimensional nanoscale structure within thin molecular films promises to create new opportunities for tailoring the physicochemical properties of surfaces. Here we report a strategy for the spontaneous formation of extremely small (2–5 nm) periodic molecular nanostructures that self-organize in solution and remain stable under ambient conditions (i.e., after removal from solution). The approach involves surface adsorption of wedge-shaped amphiphiles from a nonpolar solvent onto a solid substrate with which the adsorbate molecule has a specific favorable interaction.

To date, a few approaches have been used to create self-organized nanostructured molecular films: solution casting of diblock copolymer thin films,^{7–10} adsorbed layers of surfactants in aqueous solution (surface micelles),^{17–20} and adsorbed copolymer thin films.^{21,22} The principles behind self-assembly in these systems have been thoroughly studied and are well-understood. For example, copolymer pattern dimensions can be controlled by block length, solvent, and polymer structure. Surface micelle shape (spherical vs cylindrical) and dimension are influenced by molecular geometry and size. Periodic structures within diblock copolymer thin films have typical dimensions in the range of 10–100 nm, comparable to the current state-of-the-art for photo- or electron-beam lithography. A very recent and innovative approach, involving cast films of self-assembling dendrimers,^{23–26} results in surface patterns with repeat distances of 5–10 nm.

* To whom correspondence should be addressed. E-mail: daniel.schwartz@colorado.edu.

[†] Part of the Bob Rowell Festschrift special issue.

[‡] University of Colorado.

[§] Brookhaven National Laboratory.

- (1) Ringler, P.; Schulz, G. E. *Science* **2003**, *302*, 106.
- (2) Zhang, S. G. *Nat. Biotechnol.* **2003**, *21*, 1171.
- (3) Silva, G. A.; Czeisler, C.; Niece, K. L.; Beniash, E.; Harrington, D. A.; Kessler, J. A.; Stupp, S. I. *Science* **2004**, *303*, 1352.
- (4) Shih, W. M.; Quispe, J. D.; Joyce, G. F. *Nature* **2004**, *427*, 618.
- (5) Keren, K.; Berman, R. S.; Buchstab, E.; Sivan, U.; Braun, E. *Science* **2003**, *302*, 1380.
- (6) Yan, H.; Park, S. H.; Finkelstein, G.; Reif, J. H.; LaBean, T. H. *Science* **2003**, *301*, 1882.
- (7) De Rosa, C.; Park, C.; Thomas, E. L.; Lotz, B. *Nature* **2000**, *405*, 433.
- (8) Park, M.; Harrison, C.; Chaikin, P. M.; Register, R. A.; Adamson, D. H. *Science* **1997**, *276*, 1401.
- (9) Rockford, L.; Mochrie, S. G. J.; Russell, T. P. *Macromolecules* **2001**, *34*, 1487.
- (10) Shin, K.; Leach, K. A.; Goldbach, J. T.; Kim, D. H.; Jho, J. Y.; Tuominen, M.; Hawker, C. J.; Russell, T. P. *Nano Lett.* **2002**, *2*, 933.
- (11) Murray, C. B.; Norris, D. J.; Bawendi, M. G. *J. Am. Chem. Soc.* **1993**, *115*, 8706.
- (12) Ozin, G. A. *Acc. Chem. Res.* **1997**, *30*, 17.
- (13) Mann, S.; Archibald, D. D.; Didymus, J. M.; Douglas, T.; Heywood, B. R.; Meldrum, F. C.; Reeves, N. J. *Science* **1993**, *261*, 1286.
- (14) Firouzi, A.; Kumar, D.; Bull, L. M.; Besier, T.; Sieger, P.; Hue, Q.; Walker, S. A.; Zasadzinski, J. A.; Glinka, C.; Nicol, J.; Margolese, D.; Stucky, G. D.; Chmelka, B. F. *Science* **1995**, *267*, 1138.
- (15) Radler, J. O.; Koltover, I.; Salditt, T.; Safinya, C. R. *Science* **1997**, *275*, 810.
- (16) Wong, G. C. L.; Tang, J. X.; Lin, A.; Li, Y. L.; Janmey, P. A.; Safinya, C. R. *Science* **2000**, *288*, 2035.

(17) Wanless, E. J.; Davey, T. W.; Ducker, W. A. *Langmuir* **1997**, *13*, 4223.

(18) Ducker, W. A.; Wanless, E. J. *Langmuir* **1996**, *12*, 5915.

(19) Manne, S.; Cleveland, J. P.; Gaub, H. E.; Stucky, G. D.; Hansma, P. K. *Langmuir* **1994**, *10*, 4409.

(20) Manne, S.; Gaub, H. E. *Science* **1995**, *270*, 1480.

(21) Webber, G. B.; Wanless, E. J.; Butun, V.; Armes, S. P.; Biggs, S. *Nano Lett.* **2002**, *2*, 1307.

(22) Webber, G. B.; Wanless, E. J.; Armes, S. P.; Baines, F. L.; Biggs, S. *Langmuir* **2001**, *17*, 5551.

(23) Percec, V.; Cho, W. D.; Ungar, G.; Yeardley, D. J. P. *J. Am. Chem. Soc.* **2001**, *123*, 1302.

(24) Yoon, D. K.; Jung, H. T. *Langmuir* **2003**, *19*, 1154.

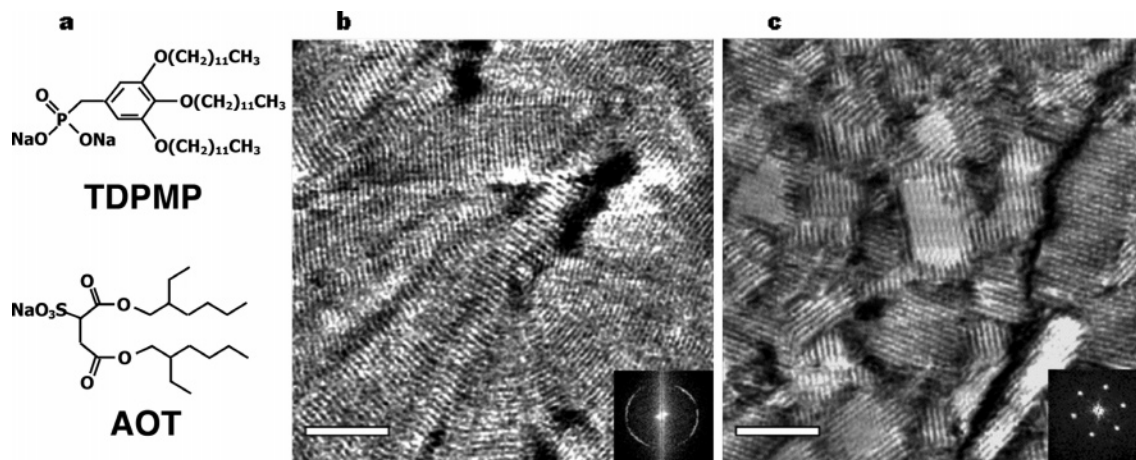


Figure 1. (a) Chemical structures of the two wedge-shaped surfactants. (b and c) Phase contrast AFM micrographs of adsorbate films imaged in air, exhibiting characteristic surface patterns. (b) Surface of adsorbed AOT film on R-sapphire after 2 h of immersion in 2.0 mM solution. The corresponding Fourier transform power spectrum is inset. Scale bar is 30 nm. (c) Surface of adsorbed TDPMP film on mica after 1 h of immersion in 1.0 mM solution and corresponding Fourier transform power spectrum (inset). Scale bar is 55 nm.

Surface micelles result in periodic arrays with a characteristic length scale of approximately 5 nm. Surface micelles also have the advantage of being an equilibrium phase, so they can be annealed to improve long-range order. However, surface micelles are stable only within the aqueous environment and the structures typically do not survive removal from solution. This limits their utility in pattern transfer applications; for example, they are incompatible with dry processes such as evaporative deposition, chemical vapor deposition, and so forth. The approach described here is closely related conceptually to that of surface micelles and results in periodic nanostructures with a similar characteristic size. The film represents an equilibrium phase and is stable under ambient conditions, making it suitable for a variety of pattern amplification methods. Moreover, the size (and, in principle, symmetry) of the surface patterns can be varied by appropriate modification of molecular architecture.

Our approach exploits the fact that the shape of a surfactant assembly is directly related to the architecture of the constituent molecules.²⁷ For example, single-chain surfactants typically form spherical micelles, while double-chain lipids form planar bilayers. Micelles and bilayers also form on solid surfaces under appropriate conditions in aqueous solution; however, these assemblies leave the hydrophilic headgroups exposed, which is not thermodynamically favorable in contact with a vapor phase, so surface micelles are disrupted during removal from aqueous solution. When the cross-sectional area of the hydrophobic region is much greater than that of the hydrophilic headgroup, reverse micelles are preferred (in nonpolar solvent). Because the hydrophobic tails are exposed in these structures, we hypothesized that surface reverse micelles could remain stable upon removal from solution. In the experiments we have performed to date, this has been true only in cases where the molecular headgroups have a specific and favorable interaction with the solid substrate. For example, wedge-shaped phosphonate amphiphiles formed a stable reverse surface

micelle phase on mica but not on silicon oxide. This behavior is consistent with observations that alkylphosphonates form planar self-assembled monolayers (SAMs) on mica^{28,29} but no stable monolayer is formed on silicon oxide. Similarly, a sulfonate-based surfactant formed a stable reverse micelle film on sapphire, but not on silicon oxide.

Experimental Details

Sodium bis-2-ethylhexylsulfosuccinate (98% purity), or AOT,³⁰ was obtained through Aldrich (Milwaukee, WI). The amphiphile disodium-3,4,5-tris(dodecyloxy)phenylmethylphosphonate, or TDPMP, was synthesized and purified as described elsewhere.³¹ Isooctane (99.9%; Fischer Scientific, Fair Lawn, NJ) was used as the solvent for self-assembly. Methanol (99.9% purity), sulfuric acid, and hydrogen peroxide were also purchased from Fischer Scientific. Water was purified with a Milli-Q UV+ purification system (Millipore, Bedford, MA). Polished sapphire wafers (diameter 2 in., thickness 0.013 in.) of R-plane sapphire (α -Al₂O₃) were purchased from Bicon (Washougal, WA). The wafers were cut into smaller pieces with a diamond scribe, cleaned in a piranha solution (~3:1 concentrated H₂SO₄/30% H₂O₂) for 20–30 min at 80–90 °C, thoroughly rinsed in Millipore water, and blown dry with nitrogen gas. The pieces were then annealed within 1 day in a nitrogen-purged muffle furnace at 1300 °C for 2 h or 1100 °C for 30 h to obtain surfaces characterized by atomically flat terraces (typically 100–300 nm wide) and steps <0.5 nm high. Once the terraces had formed, a minimum of 500 °C for 2 h was required to dehydrate the sapphire surface, enabling monolayer formation. Just before immersion, these surfaces were UV oxygen cleaned for 30 min to minimize the effect of the ambient contamination. In all cases, the sapphire pieces were used for solution adsorption within 3 days of annealing. Muscovite mica (purchased from Ted Pella, Inc., Redding, CA) was cut into 12.7 mm diameter disks and then cleaved just before immersion.

Solutions of AOT/isooctane were prepared by dissolving excess AOT (at least 100 mg) in methanol (20–30 mL) and heating the solution in a vacuum oven for a minimum of 6 h to remove any AOT-bound water. The dehydrated AOT (stored in a desiccator) was then used to make the AOT/isooctane solutions within 77 days of dehydration. TDPMP was used as received. Sonication of the TDPMP/isooctane solutions for 1 h was required for complete dissolution. Substrates were immersed in surfactant/

(25) Jung, H. T.; Kim, S. O.; Ko, Y. K.; Yoon, D. K.; Hudson, S. D.; Percec, V.; Holerca, M. N.; Cho, W. D.; Mosier, P. E. *Macromolecules* **2002**, *35*, 3717.

(26) Jung, H. T.; Kim, S. O.; Hudson, S. D.; Percec, V. *Appl. Phys. Lett.* **2002**, *80*, 395.

(27) Israelachvili, J. N. *Intermolecular and Surface Forces*, 2nd ed.; Academic Press: London, 1992.

(28) Woodward, J. T.; Ulman, A.; Schwartz, D. K. *Langmuir* **1996**, *12*, 3626.

(29) Doudevski, I.; Hayes, W. A.; Woodward, J. T.; Schwartz, D. K. *Colloids Surf., A* **2000**, *174*, 233.

(30) Zulauf, M.; Eicke, H. F. *J. Phys. Chem.* **1979**, *83*, 480.

(31) Hammond, S. R.; Zhou, W. J.; Gin, D. L.; Avlyanov, J. K. *Liq. Cryst.* **2002**, *29*, 1151.

isooctane solutions at room temperature for various times, removed, and imaged. Upon removal from solution, the surfaces were free of excess solvent.

Atomic force microscopy (AFM) imaging of adsorbed films was performed with a Digital Instruments (Santa Barbara, CA) Nanoscope III MAFM instrument, equipped with an E scanner. All images were obtained through the tapping mode using etched silicon probes (NanoDevices, Inc., Santa Barbara, CA) with fundamental resonance frequencies (f_0) of 300 kHz. These cantilevers are 125 μm in length and have a spring constant (k) of 40 N/m, width of 45 μm , and thickness of 4 μm . Phase and height (topographical) images were captured simultaneously at scan rates 1.20–2.35 Hz. Images were acquired in at least three macroscopically separated areas of each sample, and reported surface coverage and height differences are the result of the general trends found in these areas. Images were minimally flattened. The bilayer heights and domain sizes were determined from sectional analysis. The two-dimensional spectra were obtained by a Fourier transform and used to determine the spacing of the observed columnar structures.

X-ray reflectivity experiments were performed at Beamline X22 of the National Synchrotron Light Source at Brookhaven National Laboratory. Reflectivity spectra were obtained for both the clean sapphire substrate (not shown) as well as the substrate covered by TDPMP film. The reflectivity of the bare substrate showed only a gradual decay from the calculated Fresnel reflectivity, consistent with surface roughness.

Results and Discussion

Two wedge-shaped amphiphiles, AOT³⁰ and TDPMP³¹ (Figure 1a), were studied to establish a general understanding of this self-assembly phenomenon. AOT is known to form spherical reverse micelles in bulk solution.^{32,33} Parts b and c of Figure 1 show AFM images of typical surface patterns produced from adsorbed layers of AOT and TDPMP, respectively. In the case of AOT, surface structures were observed on annealed R-sapphire,³⁴ whereas TDPMP formed surface structures on mica. The structural features observed were distinctly different for each system. First of all, the repeat distances of the patterned stripes differed, and each was directly related to the molecular size of the respective amphiphile. The repeat distance of the AOT structures, determined by Fourier transform analysis (Figure 2b, inset), was 2.4 ± 0.1 nm. The molecular length of AOT is ~ 1.3 nm, so these structures are approximately two molecular lengths in size. However, they are significantly smaller than solution-phase AOT spherical reverse micelles, which have a diameter of 3.4 nm.^{32,33} It is possible that the size difference may be connected to the difference in the shape of the aggregates. The repeat distance of the TDPMP surface structures was 4.45 ± 0.15 nm which is also consistent with twice the molecular length of the molecule (~ 2.3 nm). For comparison, a sulfonic acid analogue of TDPDP has been reported to form a hexagonal lyotropic liquid crystal phase with a cylinder spacing of 4.2 nm.³⁵

The general appearance/morphology of the patterns differed for the two surfactants. The AOT surface showed meandering stripes, which produced an overall fingerprint-like texture, resembling a two-dimensional smectic liquid crystal texture. In contrast, the TDPMP layers formed relatively small crystalline domains with distinct grain boundaries. The small grain size may be related to the presence of impurities, or it may simply be a consequence

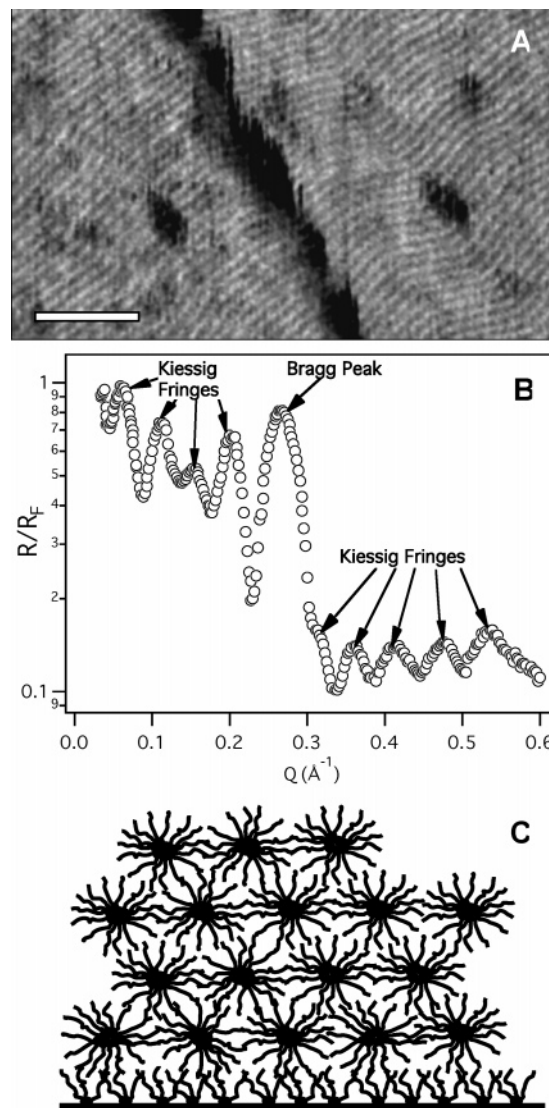


Figure 2. (a) Phase contrast AFM micrograph of adsorbed AOT film on R-sapphire after 2 h immersion in 2.0 mM isooctane solution, showing coherent stacking of structures in a multi-layered film. Scale bar is 20 nm. The corresponding height image indicates that the height of the step in this image is ~ 2.5 nm. (b) X-ray reflectivity divided by the theoretical Fresnel reflectivity. (c) Structure of a thin film of wedge-shaped molecules consistent with X-ray results and AFM observations.

of the details of the film's nucleation and growth process. The structures within a particular domain had a large degree of positional and orientation order. Analyzing the Fourier transform of the TDPMP surface reveals that the structures are oriented in three discrete directions (Figure 1c, inset), suggesting an orientational epitaxy with the hexagonal symmetry of the underlying mica surface.

Some AFM images showed the presence of surface steps with a height equal to the in-plane repeat distance (2.4 nm for AOT, 4.5 nm for TDPMP). This suggests that the films consist of stacked layers with a spacing equal to two molecular lengths. The representative image of such a step in an AOT film shown in Figure 2a also indicates that the periodic structures in adjacent layers are in register with each other. Synchrotron X-ray reflectivity experiments were performed to unambiguously determine the buried structure of the AOT film. X-ray reflectivity data (Figure 2b) showed a Bragg peak at 0.266 \AA^{-1} , corresponding to a repeat distance (unit cell) of 2.36 nm in the surface normal direction, and Kiessig fringes separated by approximately 0.060 \AA^{-1} , corresponding to

(32) Eastoe, J.; Towey, T. F.; Robinson, B. H.; Williams, J.; Heenan, R. K. *J. Phys. Chem.* **1993**, *97*, 1459.

(33) Kotlarchyk, M.; Huang, J. S.; Chen, S. H. *J. Phys. Chem.* **1985**, *89*, 4382.

(34) Taylor, C. E.; Schwartz, D. K. *Langmuir* **2003**, *19*, 2665.

(35) Resel, R.; Theissl, U.; Gadermaier, C.; Zojer, E.; Kriechbaum, M.; Amenitsch, H.; Gin, D.; Smith, R.; Leising, G. *Liq. Cryst.* **2000**, *27*, 407.

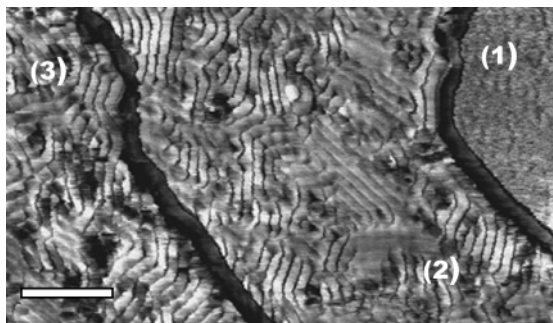


Figure 3. Phase contrast AFM micrograph of adsorbed TDPMP film on mica after 1 min of immersion in 1.0 mM isooctane solution, showing the presence of disorganized structures and multiple layers. Scale bar is 30 nm. The corresponding height image indicates that the height of the steps between distinct regions in this image is ~ 4.5 nm.

an overall film thickness of 10.5 nm, or approximately 4.5 unit cells. The second harmonic of the Bragg peak was not prominent in the data due to the details of the X-ray form factor. (Raw X-ray data are provided as Figure S.1 in Supporting Information.)

Taken together, the AFM and X-ray data are consistent with each other and with the type of structure shown in Figure 2c, with an adsorbed monolayer adjacent to the substrate followed by stacked layers of cylindrical reverse micelles. In particular, the layered nature of the structure rules out the possibility of vertically oriented lamellae.

We cannot completely rule out the possibility that the nanostructures actually represent solid crystalline films of the surfactants. However, we feel that this possibility is unlikely for several reasons. The meandering nature of the AOT stripes strongly suggests liquid crystalline behavior. Also, these wedge-shaped surfactants do not crystallize readily because of their geometry. Finally, for surfactants that do form solid crystals, the crystal structure generally resembles a lamellar structure, where only one lattice dimension is related to twice the molecular length. However, the structures observed here display a bilayer length scale in two dimensions, lateral and surface normal, consistent with the hexagonal packing of cylinders.

Observations of film structure as a function of immersion time provide interesting insight into the assembly mechanism. Figure 3 shows a TDPMP film resulting from a very short immersion time. These patterns, indicative of the early stage of growth, consist of a mixture of short rodlike shapes and roughly circular features. Correlated domains are very small, grain boundaries are not apparent, and preferred alignment is lacking. The differences in the surface morphology, between early growth and prolonged growth (Figure 1c), suggest that a self-organizing process occurs on the surface after the initial adsorption step. Figure 3 also depicts the presence of three different layers (separated by a dark shadowing artifact). Region 1 is featureless, while regions 2 and 3 show periodic nanostructures. This is consistent with the structure shown in Figure 2c, where a flat monolayer forms the

basis for the subsequent deposition and organization of cylindrical reverse micelles. Analogous stepped structures are seen in the early stages of AOT film growth. These observations are consistent with the hypothesis that an initial strongly adsorbed, dense monolayer is necessary for the subsequent formation of structured bilayers. This would require an appropriate adsorbate–substrate interaction. An appropriate criterion for the necessary headgroup–substrate interaction appears to coincide with that for the formation of a stable SAM of a single-chain adsorbate with the same headgroup. For example, just as stable alkylsulfonate SAMs form on sapphire but not mica, stable nanostructured films of AOT form on sapphire but not mica. (The details of the interaction between these organic acid adsorbates and mica or alumina are not well understood; we speculate that a Lewis acid/base interaction with aluminum ions may be involved.) Neither AOT nor TDPMP forms stable films on SiO_2 substrates, consistent with observations that stable SAMs of alkylphosphonates or alkylsulfonates also do not form on this substrate. However, it is notable that the mica and sapphire substrates are essentially atomically flat, while the silica surfaces used are amorphous. So we cannot rule out the influence of roughness and/or crystallinity on the formation of these stable nanostructured films.

Conclusions

We have demonstrated a new approach for preparing nanostructured self-organized ultrathin molecular films that remain stable under ambient conditions. The approach involves reverse micelle-forming amphiphiles (wedge-shaped) with headgroups that have a specific and favorable interaction with the chosen solid substrate. Two examples were demonstrated, one with two branched tails and one with three linear tails. In both cases, the repeat distance of the periodic nanostructures was consistent with twice the molecular length, suggesting a general strategy for tailoring the periodicity of such structures. In one case, a two-dimensional crystalline phase was observed, with domain orientations that appeared to be dictated by the crystalline axes of the underlying mica substrate. In the other case, however, a meandering “fingerprint” texture was observed, consistent with a two-dimensional smectic liquid crystal phase. This liquid crystalline phase may prove to be particularly amenable to mesoscopic alignment via interaction with lithographically defined microstructures and/or external fields.

Acknowledgment. This work was supported by National Science Foundation Award Nos. CHE-0349547 (D.K.S., C.E.T.), DMR-0213918 (M.N., N.C.), and DMR-0111193 (D.L.G. and S.R.H.). Brookhaven National Laboratory is supported by U.S. Department of Energy Contract No. DE-AC02-98CH10886.

Supporting Information Available: Raw X-ray reflectivity data of the AOT film on R-sapphire. This material is available free of charge via the Internet at <http://pubs.acs.org>.

LA050204Z